Freeze−Quench Magnetic Circular Dichroism Spectroscopic Study of the "Very Rapid" Intermediate in Xanthine Oxidase

Robert M. Jones,[†] Frank E. Inscore,[†] Russ Hille,*[,‡] and Martin L. Kirk*[,†]

Department of Chemistry, The University of New Mexico, Albuquerque, New Mexico 81731-1096, and Department of Medical Biochemistry, The Ohio State University, Columbus, Ohio 43210

Received February 5, 1999

Freeze−quench magnetic circular dichroism spectroscopy (MCD) has been used to trap and study the excited-state electronic structure of the Mo(V) active site in a xanthine oxidase intermediate generated with substoichiometric concentrations of the slow substrate 2-hydroxy-6-methylpurine. EPR spectroscopy has shown that the intermediate observed in the MCD experiment is the "very rapid" intermediate, which lies on the main catalytic pathway. The low-energy ($<\sim$30 000 cm^{-1}) *C*-term MCD of this intermediate is remarkably similar to that of the model compound LMoO(bdt) (L = hydrotris(3,5-dimethyl-1-pyrazolyl)borate; bdt = 1,2-benzenedithiolate), and the MCD bands have been assigned as dithiolate $S_{ip} \rightarrow$ Mo d_{xy} and $S_{op} \rightarrow$ Mo $d_{xz,yz}$ LMCT transitions. These transitions result from a coordination geometry of the intermediate where the Mo═O bond is oriented cis to the ene-1,2-dithiolate of the pyranopterin. Since X-ray crystallography has indicated that a terminal sulfido ligand is oriented cis to the ene-1,2-dithiolate in oxidized xanthine oxidase related *Desulfovibrio gigas* aldehyde oxidoreductase, we have suggested that a conformational change occurs upon substrate binding. The substrate-mediated conformational change is extremely significant with respect to electron-transfer regeneration of the active site, as covalent interactions between the redox-active Mo d_{xy} orbital and the S_{ip} orbitals of the ene-1,2-dithiolate are maximized when the oxo ligand is oriented cis to the dithiolate plane. This underlies the importance of the ene-1,2-dithiolate portion of the pyranopterin in providing an efficient superexchange pathway for electron transfer. The results of this study indicate that electron-transfer regeneration of the active site may be gated by the orientation of the Mo═O bond relative to the ene-1,2-dithiolate chelate. Poor overlap between the Mo d_{xy} orbital and the S_{ip} orbitals of the dithiolate in the oxidized enzyme geometry may provide a means of preventing one-electron reduction of the active site, resulting in enzyme inhibition with respect to the two-electron oxidation of native substrates.

Introduction

Xanthine oxidase is the prototypical member of the xanthine oxidase family of pyranopterin molybdenum enzymes and

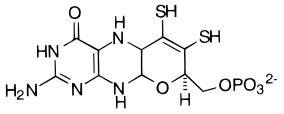

Pyranopterin

catalyzes various two-electron oxidations (hydroxylations) of purines, aldehydes, and other organic molecules. The xanthine oxidase isolated from cow's milk is a 300 kDa homodimer possessing Mo in addition to two spinach ferredoxin type iron−sulfur clusters (2Fe-2S) and flavin adenine dinucleotide (FAD) as redox cofactors. The crystal structures of a number of pyranopterin molybdenum and tungsten enzymes were recently reported.[1−5] Among these is the aldehyde oxidoreductase from *Desulfovibrio gigas*, a member of the molybdenum hydroxylase family of enzymes that includes xanthine oxidase.[3,4] The oxidized Mo center of these enzymes possesses an unusual $[Mo^{VI}OS]^{2+}$ core, with both oxo and sulfido ligands coordinated to the metal. The Mo═S group is essential for catalysis, and various mechanisms have been suggested which imply that the terminal sulfido ligand plays a functional role as either a proton or a hydride acceptor in the hydroxylation of a substrate.[6−10] The Mo active site is reduced from Mo(VI) to Mo(IV) during the reductive half-reaction of the catalytic sequence. Regeneration of the oxidized Mo(VI) site is accomplished by two sequential intramolecular one-electron transfers from the molybdenum center to 2Fe-2S clusters, to FAD, and eventually to molecular oxygen or NAD^+.[11] The detailed molecular sequence

[†] The University of New Mexico.
[‡] The Ohio State University.

(1) Schindelin, H.; Kisker, C.; Hilton, J.; Rajagopalan, K. V.; Rees, D. C. *Science* **1996**, *272*, 1615−1621.
(2) Chan, M. K.; Mukund, S.; Kletzin, A.; Adams, M. W. W.; Rees, D. C. *Science* **1995**, *267*, 1463−1469.
(3) Romão, M. J.; Archer, M.; Moura, J.; LeGall, J.; Engh, R.; Schneider, M.; Hof, P.; Huber, R. *Science* **1995**, *270*, 1170−1176.
(4) Huber, R.; Hof, P.; Duarte, R. O.; Moura, J. J. G.; Moura, I.; Liu, M.; LeGall, J.; Hille, R.; Archer, M.; Romão, M. J. *Proc. Natl. Acad. Sci. U.S.A.* **1996**, *93*, 8846−8851.
(5) Kisker, C.; Schindelin, H.; Pacheco, A.; Wehbi, W. A.; Garrett, R. M.; Rajagopalan, K. V.; Enemark, J. H.; Rees, D. C. *Cell* **1997**, *91*, 973−983.
(6) Hille, R. *Chem. Rev.* **1996**, *96*, 2757−2816.
(7) Hille, R.; Sprecher, H. *J. Biol. Chem.* **1987**, *262*, 10914.
(8) Bray, R. C.; Gutteridge, S.; Stotter, D. A.; Tanner, S. J. *Biochem. J.* **1979**, *177*, 357.
(9) Coucouvanis, D.; Toupadakis, A.; Lane, J. D.; Koo, S. M.; Kim, C. G.; Hadjikyriacou, A. *J. Am. Chem. Soc.* **1991**, *113*, 5271.
(10) Pilato, R. S.; Stiefel, E. I. In *Bioinorganic Catalysis*; Reedjik, J., Ed.; Dekker: New York, 1993; pp 131−188.
(11) The terminal electron acceptor for the oxidase form of the enzyme is molecular oxygen, while NAD^+ is used for the dehydrogenase. The two forms of the enzyme are interconvertable: Amaya, Y.; Yamazaki, K.; Sato, M.; Noda, K.; Nishino, T.; Nishino, T. *J. Biol. Chem.* **1990**, *265*, 14170.

10.1021/ic990154j CCC: $18.00
Published on Web 10/08/1999

of events underlying the reaction mechanism of the molybdenum hydroxylases continues to be an area of intense debate.

The coordination geometry of the molybdenum center in xanthine oxidase has been probed by X-ray absorption[12−18] and EPR[19−21] spectroscopies as well as inferred from its general catalytic and genetic similarity to the crystallographically defined aldehyde oxidoreductase from *D. gigas*.[3,4] The structure of the oxidized Mo active site in aldehyde oxidoreductase has been

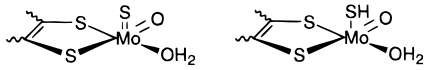

described as distorted square pyramidal with two ene-1,2-dithiolate sulfur donors, a terminal oxo, and a water (or hydroxyl) ligand forming the basal plane. Interestingly, a terminal sulfido ligand was found to occupy the apical position, cis to the dithiolate plane. A similar five-coordinate geometry was determined for the reduced Mo(IV) species. However, this is distinguishable from the oxidized Mo(VI) active site structure due to an increase in the Mo−S bond length attributed to protonation of the terminal sulfido ligand. It should be noted that the structure for the oxidized enzyme was obtained from crystals soaked in sulfide and that the structure for the reduced enzyme was obtained on a chemically rather than catalytically reduced species.[4] A Mo(V) state giving rise to a distinctive EPR signal, designated "very rapid" on the basis of the millisecond time scale on which it is observed in the course of the reaction of the enzyme with xanthine, has also been described[22] in addition to the Mo(VI) and Mo(IV) states involved in the reductive half-reaction. This EPR signal accumulates to a significant degree in the course of enzyme turnover with the slow substrate 2-hydroxy-6-methylpurine[22] and has been shown to lie along the main catalytic pathway.[6,23] Significant concentrations of the paramagnetic molybdenum−product (Mo(V)−P) intermediate,[24] giving rise to the "very rapid" EPR signal, can be generated under appropriate conditions[23] without the concomitant production of other paramagnetic chromophores (namely, reduced 2Fe-2S clusters and FADH•). Thus, it has become possible for the first time to study the xanthine oxidase Mo(V) site in detail by magnetic circular dichroism (MCD) spectroscopy and gain additional insight into the geometric and electronic structure of this key catalytic intermediate.

The intense UV/visible absorption of xanthine oxidase arises from the 2Fe-2S clusters and FAD, severely obscuring the weak contributions to the electronic absorption spectrum arising from the Mo site. As a result, few excited-state studies of the Mo center in xanthine oxidase have been attempted[25−28] and much of our current knowledge regarding the electronic structure of this site has been provided by EPR,[19−21,29,30] ENDOR,[31−33] and ESEEM[34] studies of paramagnetic Mo(V) species generated under a variety of reaction conditions. While these studies have yielded important information about the nature of the ground-state wave function, complementary studies of the excited-state electronic structure, which directly probe covalency contributions to active site reactivity, have not been undertaken. Hence, many of the key electronic structure factors which contribute to enzyme catalysis remain to be determined. MCD spectroscopy is a selective and sensitive probe of both ground- and excited-state properties of paramagnetic intermediates, and the technique has been used to study desulfo-inhibited xanthine oxidase[28] and the DMSO reductases from *R. sphaeroides* and *R. capsulatus*,[35,36] in addition to synthetic small-molecule analogues of their active sites.[37,38] We have employed an extension of this technique, namely freeze−quench difference magnetic circular dichroism spectroscopy, to trap the xanthine oxidase "very rapid" intermediate and probe the excited-state electronic structure of the Mo(V) site under turnover conditions. When interpreted in the context of structurally and spectroscopically defined model compounds, this excited-state spectral information affords an unprecedented opportunity to develop a detailed understanding of electronic and geometric structure contributions to reactivity, which include the mode of product binding, the nature of the pyranopterin ene-1,2-dithiolate interaction with Mo, and the role of the this moiety in electron-transfer regeneration of the active site following substrate hydroxylation.

Experimental Section

1. Preparation of the Xanthine Oxidase/Hydroxymethylpurine Mo(V) Catalytic Intermediate. The methodology described in the following subsection is an adaptation of that developed by Hille[23] for production of the Mo(V) species exhibiting the "very rapid" EPR signal observed under turnover conditions. The as-isolated oxidized bovine xanthine oxidase in 0.1 M pyrophosphate buffer at pH 8.5 was found to be 90% functional. The 10% inactive component found in most preparations of xanthine oxidase lacks the catalytically essential sulfido ligand at the Mo center (desulfo xanthine oxidase). The enzyme used in preparing the "very rapid" intermediate was exchanged into a reaction buffer composed of 0.1 M 3-(cyclohexylamino)propanesulfonic acid (CAPS), 0.1 M KCl, and 0.3 mM EDTA at pH 10 using a PD-10 (Pharmacia) gel filtration column. The buffer-exchanged xanthine

(12) Tullius, T. D.; Durtz, D. M., Jr.; Conradson, S. D.; Hodgson, K. O. *J. Am. Chem. Soc.* **1979**, *101*, 2776.
(13) Bordas, J.; Bray, R. C.; Garner, C. D.; Gutteridge, S.; Hasnain, S. *Biochem. J.* **1980**, *191*, 499.
(14) Cramer, S. P.; Wahl, R.; Rajagopalan, K. V. *J. Am. Chem. Soc.* **1981**, *103*, 7721.
(15) Cramer, S. P.; Hille, R. *J. Am. Chem. Soc.* **1985**, *107*, 8164.
(16) Hille, R.; Georger, G. N.; Eidsness, M. K.; Cramer, S. P. *Inorg. Chem.* **1989**, *28*, 4018.
(17) Turner, N. A.; Bray, R. C.; Diakun, G. P. *Biochem. J.* **1989**, *260*, 563.
(18) Cramer, S. P. *Adv. Inorg. Bioinorg. Mech.* **1983**, *2*, 259.
(19) Malthouse, J. P.; George, G. N.; Lowe, D. J.; Bray, R. C. *Biochem. J.* **1981**, *199*, 629−637.
(20) George, G. N.; Bray, R. C. *Biochemistry* **1988**, *27*, 3603−3609.
(21) Greenwood, R. J.; Wilson, G. L.; Pilbrow, J. R.; Wedd, A. G. *J. Am. Chem. Soc.* **1993**, *115*, 5385−5392.
(22) Bray, R. C.; Vanngard, T. *Biochem. J.* **1969**, *114*, 725.
(23) McWhirter, R. B.; Hille, R. *J. Biol. Chem.* **1991**, *266*, 23724.
(24) P is defined as the product 2,8-dihydroxy-6-methylpurine coordinated to the molybdenum via the catalytically introduced hydroxyl group at position 8.
(25) Ryan, M. G.; Ratnam, K.; Hille, R. *J. Biol. Chem.* **1995**, *270*, 19209.
(26) Hille, R.; Stewart, R. C. *J. Biol. Chem.* **1984**, *259*, 1570.
(27) Kim, J. H.; Hille, R. *J. Biol. Chem.* **1993**, *268*, 44.
(28) Peterson, J.; Godfrey, C.; Thomson, A. J.; George, G. N.; Bray, R. C. *Biochem. J.* **1986**, *233*, 107−110.
(29) Tanner, S. J.; Bray, R. C.; Bergmann, F. *Biochem. Soc. Trans.* **1978**, *6*, 1328.
(30) George, G. N.; Bray, R. C. *Biochemistry* **1988**, *27*, 3603.
(31) Howes, B. D.; Bray, R. C.; Richards, R. L.; Turner, N. A.; Bennett, B.; Lowe, D. J. *Biochemistry* **1996**, *35*, 1432.
(32) Howes, B. D.; Pinhal, N. M.; Turner, N. A.; Bray, R. C.; Anger, G.; Ehrenberg, A.; Raynor, J. B.; Lowe, D. J. *Biochemistry* **1990**, *29*, 6120.
(33) Howes, B. D.; Bennett, B.; Bray, R. C.; Richards, R. L.; Lowe, D. J. *J. Am. Chem. Soc.* **1994**, *116*, 11624.
(34) Lorigan, G. A.; Britt, R. D.; Kim, J. H.; Hille, R. *Biochim. Biophys. Acta* **1994**, *284*, 1185.
(35) Benson, N.; Farrar, J. A.; McEwan, A. G.; Thompson, A. J. *FEBS Lett.* **1992**, *307*, 169−172.
(36) Finnegan, M. G.; Hilton, J.; Rajagopalan, K. V.; Johnson, M. K. *Inorg. Chem.* **1993**, *32*, 2616−2617.
(37) Carducci, M. D.; Brown, C.; Solomon, E. I.; Enemark, J. H. *J. Am. Chem. Soc.* **1994**, *116*, 11856−11868.
(38) Inscore, F. E.; McNaughton, R.; Westcott, B. L.; Helton, M. E.; Jones, R.; Dhawan, I. K.; Enemark, J. H.; Kirk, M. L. *Inorg. Chem.* **1999**, *38*, 1401−1410.

oxidase solution was centrifuged for 10 min to remove any insoluble material and degas the solution. The enzyme concentration was determined to be 440 μM using the molar extinction coefficient of 37.8 mM^{-1} cm^{-1} at 450 nm. The slow-reacting substrate 2-hydroxy-6-methylpurine (HMP) was prepared at 20 mM in this reaction buffer, and the xanthine oxidase and HMP solutions were subsequently stored on ice. Solubility tests demonstrated that the enzyme would precipitate from solution upon mixing with neat PEG-400. This problem was avoided by preparing the PEG-400 as a 66% (v/v) solution in the reaction buffer. The poor buffering capacity of CAPS required that the PEG solution be initially titrated with NaOH to raise the pH to 10. This solution was degassed by repeated freeze−pump−thaw cycles and stored on ice.

Reactions were carried out in 1.0 mL BioFreeze (CoStar) vials encased in ice. A 673-μL sample of the buffered 66% PEG-400 solution was gently transferred into the reaction vial, with care being taken not to entrain air into the solution. After this solution settled in the bottom of the reaction vial, 321 μL (282 μM total Mo(VI) and 254 μM active Mo(VI)) of the xanthine oxidase solution was gently layered on top of the PEG-400 solution. Substrate catalysis was initiated by introducing 6.3 μL (141 μM) of HMP solution into the top xanthine oxidase containing layer. The vial was then gently swirled for a few seconds while remaining in the ice bath and then allowed to stand undisturbed for 30 s. The two separated layers were then rapidly mixed together using a cold (0 °C) glass stirring rod. Once homogenized, the reaction solution was rapidly poured into a glass syringe, and the optical cell was filled and then immediately plunged into a shallow liquid-nitrogen-filled dewar to quench the reaction and glass the solution. The total time elapsed from introduction of substrate to quenching in liquid nitrogen was 68 s. While immersed in liquid nitrogen, the sample cell was threaded onto the end of the cryostat sample rod and quickly transferred into the 80 K sample space of an Oxford Instruments SMT-4000 superconducting magnet. The final concentration of xanthine oxidase combined with the 1.5 mm cell path length results in an absorption of 0.8 at 450 nm. Maximum signal to noise for our MCD experiments is obtained with samples possessing an absorption between 0.5 and 1.2.

2. Preparation of Oxidized Mo(VI) Xanthine Oxidase. The same PEG-400 and xanthine oxidase stock solutions employed in the preparation in the Mo(V)−P intermediate were used to prepare the oxidized enzyme sample. A 1.0 mL BioFreeze vial was charged with 160 μL of enzyme solution and 336 μL of the 66% PEG-400 solution. The sample was then thoroughly mixed, and the optical cell was filled by the methods outlined previously. An optical glass was formed by immersing the sample cell in liquid nitrogen prior to mounting on the cryostat sample rod.

3. Preparation of Fully Reduced Mo(IV) Xanthine Oxidase. The aerobic xanthine oxidase−HMP reaction kinetics of Hille[23] demonstrated that redox equivalents do not accumulate in the 2Fe-2S clusters or FAD. However, these studies were conducted on aqueous buffered solutions devoid of the PEG-400 cryoprotectant required for low-temperature MCD studies. The high viscosity of the PEG-400 reaction solutions was anticipated to retard the mass-transfer rates during catalysis which, combined with the thorough degassing of the reactant solutions prior to mixing, lead to the possibility that additional redox equivalents might have been present in the Mo(V)−P intermediate sample. Therefore, it was essential to ascertain the *C*-term MCD spectral signature of reduced 2Fe-2S clusters, since Mo(IV) and $FADH_2$ are diamagnetic and do not contribute to the temperature-dependent *C*-term component of the MCD spectrum. An aliquot of the xanthine oxidase/PEG-400 reaction buffer solution was fully reduced by adding solid sodium dithionite to the solution, and the concomitant bleaching of the visible absorption was monitored spectophotometrically. An additional amount of sodium dithionite was added to this solution to ensure the redox centers remained fully reduced during the time required to load the sample in the MCD cell and glass the solution in liquid nitrogen.

4. Preparation of LMoO(bdt). The Mo(V) model compound, LMoO(bdt) (L = hydrotris(3,5-dimethyl-1-pyrazolyl)borate; bdt = 1,2-benzenedithiolate), was prepared as previously described[39,40] in an inert atmosphere of nitrogen using standard Schlenk techniques. All solvents were distilled and deoxygenated prior to use. Purification of solvents was accomplished using the following methodologies: triethylamine from potassium hydroxide; toluene, from sodium benzophenone. Other solvents were used without further purification.

5. Freeze−Quench Difference Magnetic Circular Dichroism Spectroscopy. All MCD spectra were acquired on samples loaded into a custom-designed, brass microcell. This cell incorporates a nominal 1.5 mm notched silicon O-ring interspersed between two removable Infrasil quartz windows. The sample cell was designed to be quickly threaded onto the MCD sample rod. The cell was loaded through a narrow-bore hole designed to accommodate a fine-gauge syringe. A 1.0 mL glass syringe was affixed with a 23 gauge stainless steel needle and fitted into the sample cell prior to filling the cell. This entire sample cell assembly, minus the top of the syringe plunger, was wrapped in Parafilm and then packed in ice and allowed to equilibrate.

The MCD spectrometer is built around a Jasco J-600 spectropolarimeter interfaced to an IBM AT computer and an Oxford Instruments Spectromag 4000-7 split-coil superconducting magnet system.[38] Extensive calibration of both the spectropolarimeter and the cryostat was carried out prior to data acquisition. It is essential to verify that the sample is optically isotropic and free of strain birefringence in MCD experiments involving optical glasses. Therefore, before commencing with an MCD experiment, we tested each sample for depolarization. This was accomplished by comparing the intrinsic circular dichroism of an L-nickel tartrate solution placed in front of and then in back of the enzyme sample which was residing at 80 K in the magnetooptical cryostat. Xanthine oxidase samples exhibit substantial intrinsic circular dichroism arising from the 2Fe-2S clusters, and this adds to that of the L-nickel tartrate solution. The maximum difference between the two L-nickel tartrate solution circular dichroism spectra was less than 5% for all samples in this study.

The high-temperature MCD spectra of the Mo(V)−P intermediate were obtained at 80 ± 1 K in an applied magnetic field of 7 T. One data set was collected with the applied field in the positive direction; then the field was reversed and a second MCD spectrum was collected. These two spectra contain contributions from the natural CD and MCD of the enzyme. The natural CD derives from the 2Fe-2S clusters while the MCD is composed of two parts: one being the universal diamagnetic (*B*-term) dispersion and the other owing to the presence of paramagnetic (*C*-term) species.[41] To improve the signal-to-noise ratio, the MCD spectrum was obtained by subtracting the −7 T from the +7 T spectrum and dividing the result by 2, since the matrix elements for the natural CD are independent of the magnetic field direction while those for the MCD change sign with the direction of the field as defined by its relation to the propagation vector for the incident circularly polarized electromagnetic wave.[42] The high-temperature (80 K) spectrum contains overwhelmingly dominant contributions from the temperature-independent (*B*-term) MCD,[41] which primarily derives from the oxidized 2Fe-2S clusters. Temperature-dependent *C*-term contributions to the MCD are very small at 80 K in a 7 T applied magnetic field. This results from the fact that the two components of an $m_s = \pm 1/2$ Kramers doublet (Mo(V) and reduced 2Fe-2S clusters are $S_T = 1/2$ species) are essentially equally populated at 80 K. The temperature-dependent *C*-term contributions to the MCD predominate at 4.7 K. Therefore, the 4.7 K minus 80 K MCD difference spectrum represents the pure temperature-dependent *C*-term MCD originating from the Mo(V)−P enzyme intermediate in addition to any residual paramagnetism arising from reduced 2Fe-2S clusters and/or the $FADH^{\bullet}$ radical. The MCD spectrum of the Mo(V)−P intermediate was obtained by interactive spectral subtraction of the *C*-term MCD for the oxidized and reduced xanthine oxidase preparations.

6. EPR Spectroscopy of the Mo(V)−P Intermediate. The Mo(V)−P intermediate sample was removed from the MCD sample holder under

(39) Dhawan, I. K.; Pacheco, A.; Enemark, J. H. *J. Am. Chem. Soc.* **1994**, *116*, 7911−7912.
(40) Dhawan, I. K.; Enemark, J. H. *Inorg. Chem.* **1996**, *35*, 4873−4882.
(41) Piepho, S. B.; Schatz, P. N. *Group Theory in Spectroscopy with Applications to Magnetic Circular Dichroism*; Wiley-Interscience: New York, 1983.
(42) Stephens, P. J. *J. Chem. Phys.* **1970**, *52*, 3489−3516.

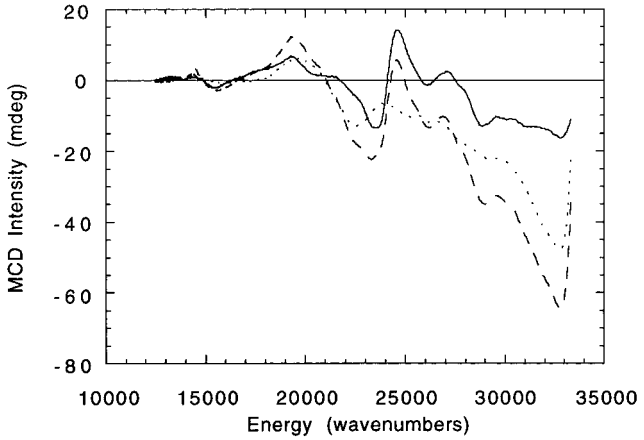

Figure 1. MCD spectra of the xanthine oxidase intermediate preparation. Data were collected at 80 K (dotted), 4.8 K (dashed), and 4.7 K minus 80 K (solid).

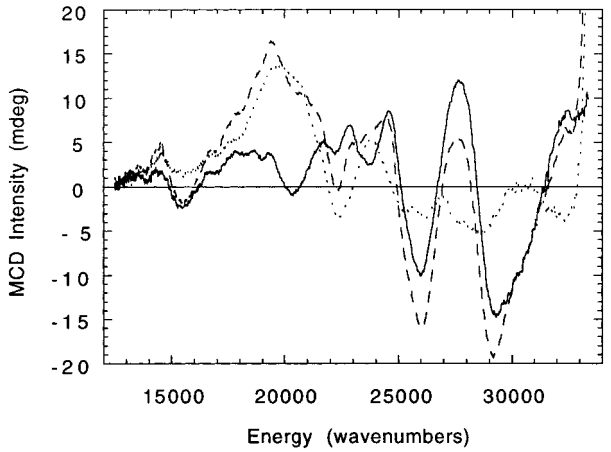

Figure 2. Temperature-dependent MCD spectra of "as-isolated" aerial-oxidized xanthine oxidase. Data were collected at 80 K (dotted), 4.8 K (dashed), and 4.7 K minus 80 K (solid).

liquid N_2, and the frozen solution was placed in an EPR tube. EPR spectra were recorded on a Bruker ER300 spectrometer equipped with an ER035M NMR gaussmeter and a Hewlett-Packard 532B microwave frequency counter. The X-band ($\sim$0.31 cm^{-1}) spectrum was acquired at 150 K, using 10 mW of power tuned at the cavity resonance frequency of 9.47 GHz. Double-spin integration of the EPR spectrum was performed to quantify the amount of Mo(V) present in the sample.

Results

The 80 K, 4.7 K, and 4.7 K minus 80 K difference MCD spectra of the xanthine oxidase intermediate preparation are presented in Figure 1. The difference spectrum represents the pure *C*-term contribution to the total MCD dispersion. This temperature-dependent *C*-term spectrum results from chromophores possessing paramagnetic ground states. In addition to the anticipated Mo(V)−P catalytic intermediate giving rise to the "very rapid" EPR signal, reduced forms of the other canonical redox cofactors (reduced 2Fe-2S clusters and the FAD$^{\bullet}$ semiquinone radical) are possible contributors to the *C*-term MCD spectrum. Therefore, the observed temperature-dependent spectral features cannot initially be ascribed solely to the presence of the Mo(V)−P intermediate.

The temperature-dependent MCD spectra of aerial-oxidized xanthine oxidase is shown in Figure 2. Again, the presence of temperature-dependent *C*-terms is direct evidence of paramagnetic species which are present a priori in the stock enzyme solution. Fully oxidized active enzyme should be diamagnetic

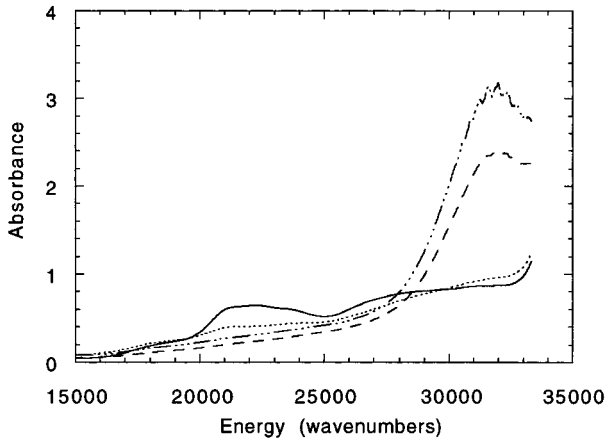

Figure 3. Absorption spectra depicting the reductive titration of xanthine oxidase with $Na_2S_2O_4$ (solid line, oxidized sample; dashed line, enzyme reduced with 2 mg of $Na_2S_2O_4$; dotted−dashed line, enzyme reduced with excess $Na_2S_2O_4$) and the spectrum 14 h following the slow aerobic reoxidation of the cofactors by diffusion of dioxygen (dotted line). The enzyme concentration is 140 μM.

and is not anticipated to yield a temperature-dependent *C*-term spectrum. Thus, the 80 and 4.8 K spectra should be superimposable. However, this is not observed and the temperature dependence present in Figure 2 must derive from one or more single-electron-reduced cofactors of the enzyme. Except for the presence of low-intensity bands occurring below 16 000 cm^{-1}, the *C*-term spectra in Figures 1 and 2 share no common features. This indicates that the *C*-term spectrum shown in Figure 1 results from a superposition of spectral components originating from at least two paramagnetic chromophores.

The absorption spectra of xanthine oxidase are dominated by contributions from the 2Fe-2S clusters and FAD. The absorption spectra in Figure 3 reflect the reductive titration of xanthine oxidase by sodium dithionite, and the bleaching of the visible absorption concomitant with the formation of reduced 2Fe-2S clusters and $FADH_2$ is clearly evident. The three xanthine oxidase cofactors are reduced as follows:[43]

$$\text{Fe(III)}-\text{Fe(III)} + e^- \rightarrow \text{Fe(II)}-\text{Fe(III)}$$

$$\text{FAD} + 2e^- + 2H^+ \rightarrow \text{FADH}_2$$

$$\text{Mo(VI)} + 2e^- \rightarrow \text{Mo(IV)}$$

Of these three reduced species, only the 2Fe-2S clusters are paramagnetic. Both the Mo(IV) center and $FADH_2$ are diamagnetic, and the reduced 2Fe-2S cluster paramagnetism ($S_T = {}^1/_2$) results from the strong antiferromagnetic exchange coupling between Fe(II) ($S = 2$) and Fe(III) ($S = {}^5/_2$) centers within each dimer.[44] Also depicted in Figure 3 is the slow aerobic reoxidation of the cofactors by diffusion of dioxygen, the terminal electron acceptor for the reduced $FADH_2$ site in the enzyme.

Figure 4 shows the MCD spectra of the dithionite-reduced xanthine oxidase preparation. The intense temperature-dependent *C*-term spectrum is characteristic of reduced 2Fe-2S clusters with ground-state spin $S_T = {}^1/_2$. Early work utilized the unique EPR spectrum of the reduced 2Fe-2S clusters[45,46] in xanthine oxidase to demonstrate their presence and unambiguously assign the temperature-dependent MCD observed as arising from these

(43) Hille, R. *Biochim. Biophys. Acta* **1994**, *1184*, 143−169.
(44) Spencer, J. T. *Coord. Chem. Rev.* **1983**, *48*, 59−82.
(45) Hille, R.; Hagen, W. R.; Dunham, W. R. *J. Biol. Chem.* **1985**, *260*, 10569−10575.
(46) Hille, R.; Gewirth, A. Private communication.

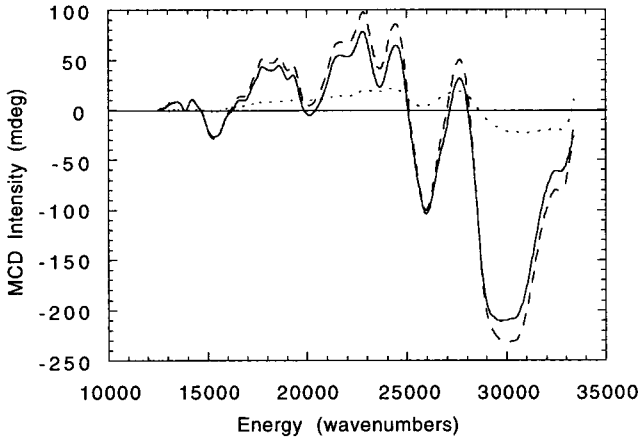

Figure 4. Temperature-dependent MCD spectra of $Na_2S_2O_4$-reduced xanthine oxidase. Data were collected at 80 K (dotted), 4.8 K (dashed), and 4.7 K minus 80 K (solid). The enzyme concentration is 140 μM.

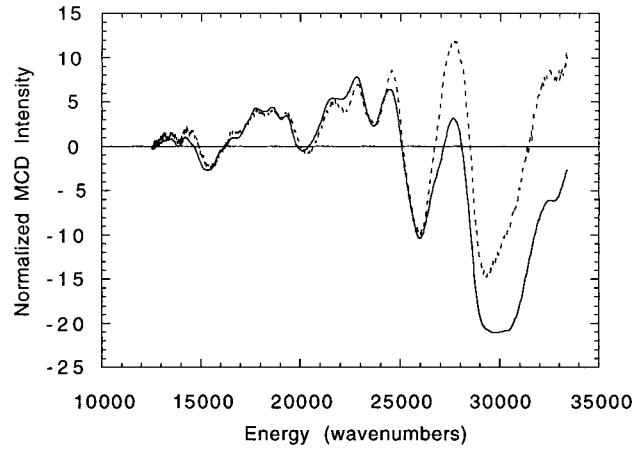

Figure 5. Comparison of the temperature-dependent MCD spectra of oxidized (dashed) and $Na_2S_2O_4$-reduced (solid) xanthine oxidase. The enzyme concentration is 140 μM.

paramagnetic centers. Figure 5 shows an overlay of the normalized *C*-term spectra from oxidized xanthine oxidase and dithionite-reduced xanthine oxidase. These spectra exhibit virtually identical spectral features, which differ only in the relative intensities of the highest energy ($>24\,000$ cm^{-1}) transitions. It is possible that the spectral differences at high energy are attributable to absorption from paramagnetic ($S = {}^1/_2$) $SO_2^{\bullet}$, which derives from the homolytic cleavage of dithionite ($S_2O_4^{2-}$) known to occur in aqueous solutions.

The overall MCD spectral similarities between oxidized and dithionite-reduced xanthine oxidase preparations indicate that the oxidized sample contains a small, but measurable, quantity of paramagnetic reduced 2Fe-2S clusters. Knowledge of the oxidized and reduced enzyme concentrations, and their respective MCD intensities, allows one to calculate the approximate percentage of *reduced* 2Fe-2S clusters present in the oxidized xanthine oxidase sample. This value is determined to be $3.5 \pm 0.5\%$.

The reduced enzyme component present in the oxidized xanthine oxidase sample is catalytically unreactive to the HMP substrate and is therefore present at the same concentration in the intermediate sample. As a result, the contribution of reduced enzyme to the *C*-term MCD spectrum of the intermediate can be removed by spectral subtraction, and this is shown in Figure 6. The resulting *C*-term difference spectrum originates solely from electronic transitions arising from the Mo(V) center in the enzyme. As such, this represents the first MCD spectrum

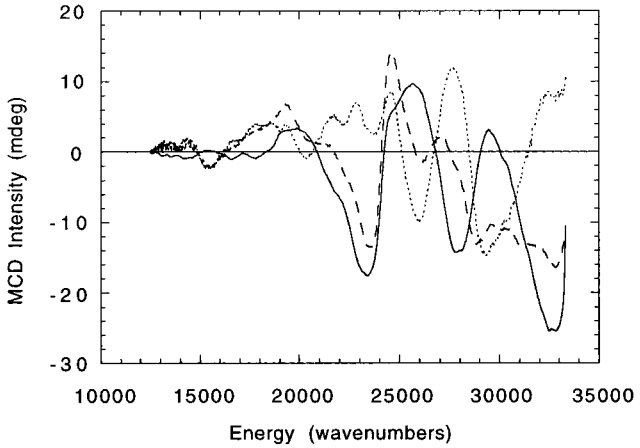

Figure 6. Temperature-dependent MCD spectrum of the "very rapid" Mo(V)−P center of xanthine oxidase (solid) obtained by subtraction of the temperature-dependent oxidized spectrum (dotted) from the temperature-dependent spectrum of the xanthine oxidase intermediate preparation (dashed). The enzyme concentration is 140 μM.

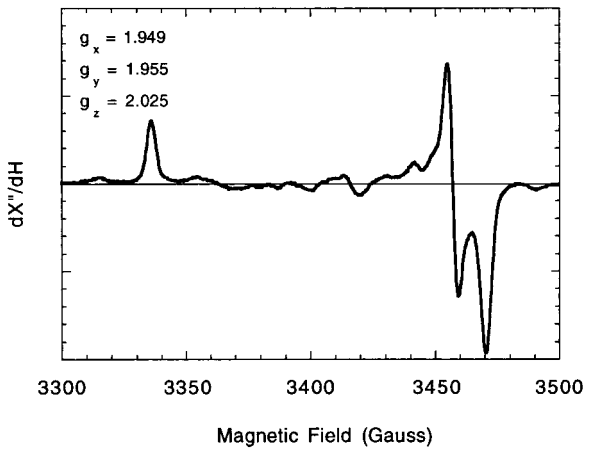

Figure 7. X-band EPR spectrum of the "very rapid" MCD sample. Data were acquired at 150 K, 9.47 GHz, and 10 mW microwave power. The integrated signal intensity corresponded to a total Mo(V) spin concentration of 147 μM. The enzyme concentration is 140 μM (254 μM in active Mo). The concentration of HMP is 141 μM, implying essentially quantitative conversion to Mo(V) under substrate-limiting conditions.

obtained for the "very rapid" catalytic intermediate trapped under turnover conditions. There is some uncertainty in the effective sample concentration, defined as the product of the enzyme concentration and optical path length, since the path length is known to change slightly upon freezing the sample. Therefore, a reasonable range of weights was applied to the oxidized xanthine oxidase *C*-term spectrum and subtracted from the intermediate *C*-term spectrum. Despite very small changes in the relative intensities of observed bands, the number of MCD features and their respective band shapes remain essentially unchanged by this procedure.

Immediately following the collection of the MCD data, the xanthine oxidase intermediate sample was removed from the MCD sample cell under liquid N_2 and placed in an EPR tube. The EPR spectrum of the intermediate is shown in Figure 7 and is identical to previously published spectra of the "very rapid" intermediate arising from Mo(V).[19−21,29,30] Double integration of the EPR intensity places the Mo(V) concentration at $\sim$147 μM. The concentration of substrate in the intermediate sample preparation was 141 μM (substrate-limiting conditions) prior to freeze-quenching the reaction. Thus, the spin integration

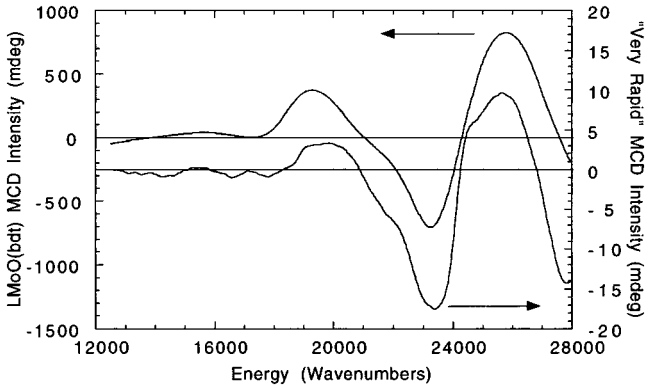

Figure 8. Comparison of the MCD spectrum from the Mo(V)−product-bound xanthine oxidase intermediate (right) at 4.7 K/7 T with the solid-state mull MCD spectrum of LMoO(bdt) in poly(dimethylsiloxane) (left) at 4.86 K/7 T. The enzyme concentration is 140 μM.

results suggest that a quantitative oxidation of substrate occurred in the reaction of oxidized enzyme with HMP in PEG-400. This implies that ~60% (147 μM out of 254 μM) of the Mo sites in the intermediate preparation exist in the Mo(V) oxidation state.

Discussion

Freeze−quench difference MCD spectroscopy has been used for the first time to probe the excited-state electronic structure of a non-oxygen enzyme intermediate, the "very rapid" intermediate in the reaction mechanism of xanthine oxidase. The paramagnetic *C*-term MCD, deriving solely from the Mo center, was presented in Figure 6. Detailed spectral comparison of the MCD originating from this intermediate with that obtained on well-defined model compounds permits the determination of pivotal relationships between the geometric and electronic structures of the active site. The first coordination sphere of the minimal active site model, LMoO(bdt), consists of three nitrogen donors from the spectroscopically innocent ligand L (L = hydrotris(3,5-dimethyl-1-pyrazolyl)borate), and a terminal oxo ligand oriented cis to the coordinated dithiolate (bdt = 1,2-benzenedithiolate):

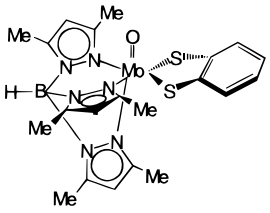

The success of the effective spectroscopic model approach is clearly evident in a comparison of the MCD spectrum of the enzyme intermediate with that of the model, and this is given in Figure 8. A remarkably close correspondence in spectral features is observed over the entire energy range shown. This is very surprising, since the X-ray structure of oxidized xanthine oxidase related aldehyde oxidoreductase from *D. gigas* shows that a terminal sulfido ligand is oriented cis to the ene-1,2-dithiolate chelate and cis to a terminal oxo ligand. The concurrence of spectral features over such a large energy range can only be the result of nearly identical manifolds of excited states. This is important, since the energy and electronic description of each individual excited state derives from the nature of the metal−ligand bonding as well as the stereochemical arrangement of the donor ligands at the molybdenum site. Thus, an understanding of electronic structure contributions to catalysis and electron-transfer regeneration in the xanthine oxidase family of pyranopterin molybdenum enzymes emerges from a description of the origin of the excited-state spectral features present in the "very rapid" intermediate generated under turnover conditions.

We recently undertook a detailed electronic absorption, resonance Raman, and MCD spectroscopic study of a series of LMoO(S-S) complexes,[47] including the model compound LMoO(bdt).[38] Our work conclusively determined that all of the observed transitions below ~30 000 cm^{-1} derive from ligand-to-metal charge transfer (LMCT) transitions originating from filled, predominantly sulfur-containing orbitals of the coordinated dithiolate ligand. Resonance Raman excitation profiles of the 19 000 cm^{-1} *C*-term and the pseudo-*A*-terms[48] at 22 000 and 24 000 cm^{-1} display selective normal-mode enhancement consistent with a highly anisotropic bonding description.[38] The assignment of the 19 000 cm^{-1} band as an in-plane dithiolate $S_{ip} \rightarrow$ Mo d_{xy} LMCT transition was based on the resonance enhancement of highly coupled in-plane Mo−S stretching and bending modes. Additionally, the assignment of the higher energy LMCT transitions (22 000 and 24 000 cm^{-1} bands) as an out-of-plane dithiolate $S_{op} \rightarrow$ Mo $d_{xz,yz}$ transition is consistent with their pseudo-*A*-term MCD band shapes and resonance enhancement of the high-frequency Mo═O stretch accompanying excitation into these bands. Given the strong correlation in MCD spectral features of LMoO(bdt) and the enzyme, we apply the same spectral assignments to the "very rapid" intermediate.

An important consequence of the MCD spectral similarity between LMoO(bdt) and the "very rapid" intermediate is the definitive determination of the stereochemical relationship between the Mo═O bond and the coordinated ene-1,2-dithiolate portion of the pyranopterin as well as the importance of the electronic structural consequences of this geometry to catalysis and electron-transfer regeneration of the active site. Since the Mo═O bond is oriented cis to the dithiolate chelate in LMoO(bdt), while crystallography indicates it is the terminal sulfido (Mo═S) ligand which is oriented cis to the ene-1,2-dithiolate plane in oxidized xanthine oxidase related aldehyde oxidoreductase, we propose that a change in Mo coordination geometry occurs during catalysis.[49] This conformational change is depicted in the mechanistic sequence presented in Scheme 1. The starting point in catalysis is the Mo(VI) resting form of the enzyme (**A**), which is fully competent to bind substrate and possesses the coordination geometry derived from the crystal structure study. Kinetic studies indicate that binding of the substrate and product release from the reduced enzyme are two-step processes.[26,50,51] Thus, the initial catalytic event may be envisioned as either a covalent or a noncovalent association of

(47) (S-S) represents a dithiolate chelate which forms a five-membered chelate ring with Mo.

(48) A positive pseudo-*A*-term is a derivative-shaped MCD feature with the positive component at higher energy. The pseudo-*A*-term changes sign at a point which corresponds to the band maximum in an electronic absorption spectrum.

(49) Recent theoretical studies (Voityuk, A. A.; Albert, K.; Köstlmeier, S.; Nasluzov, V. A.; Neyman, K. M.; Hof, P.; Huber, R.; Romão, M. J.; Rösch, N. *J. Am. Chem. Soc.* **1997**, *119*, 3159; *Inorg. Chem.* **1998**, *37*, 176) indicate that the stable conformer has the oxo ligand in the apical position, oriented cis to the ene-1,2-dithiolate. However, these are *gas-phase* calculations which lack any charge/steric contributions from amino acid residues located in the vicinity of the active site. The conformational change we are referring to need not represent a large physical change in the molybdenum coordination geometry (Scheme 4, **A** → **B**). This reoganizational barrier has been calculated to be as low as 0.5 kcal/mol (Ilich, P.; Hille, R. *J. Phys. Chem.* **1999**, *103*, 5406−5412).

(50) Davis, M. D.; Olson, J. S.; Palmer, G. J. *J. Biol. Chem.* **1982**, *257*, 14730−14737.

(51) Bray, R. C. *Adv. Enzymol. Relat. Areas Mol. Biol.* **1980**, *51*, 107.

Scheme 1

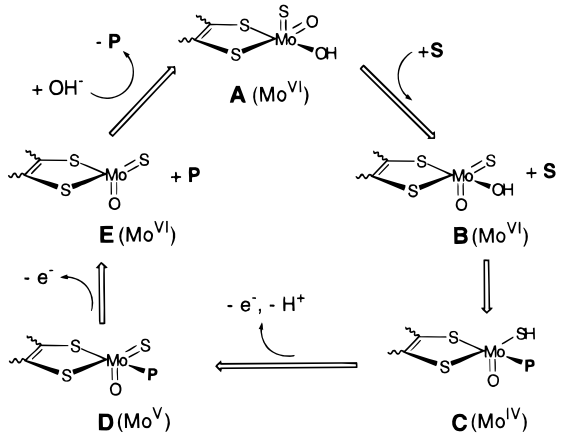

the substrate at the active site which triggers a conformational change at the Mo center and drives the oxo ligand out of the ene-1,2-dithiolate plane and into a position normal to it (**B**) yielding the MoO(dithiolate) stereochemistry observed in the model compound LMoO(bdt). The second step in the binding process results in hydroxylation of the substrate and concomitant reduction of the active site to Mo(IV) (**C**). The conformational change induced by the substrate is extremely significant with respect to electron-transfer regeneration of Mo(IV) to the fully oxidized Mo(VI) state (**D** and **E**). Covalent interactions between the redox-active Mo d_{xy} orbital and the S_{ip} orbitals of the dithiolate are maximized when the oxo ligand is oriented cis to the dithiolate plane,[38] underlying the importance of the ene-1,2-dithiolate portion of the cofactor in catalysis. Furthermore, there is mounting evidence that efficient coupling of the reduced Mo site into protein-mediated superexchange pathways[38] is facilitated by the pyranopterin, as the structure of *D. gigas* aldehyde oxidoreductase shows the amino group of the pterin hydrogen-bonded to a cysteinyl sulfur of a 2Fe-2S cluster.[3,4] We hypothesize that the presence of substrate/product at the active site maximizes the magnitude of the electron-transfer coupling matrix element (H_{DA}) between donor and acceptor sites by virtue of a conformationally induced increase in covalent interactions between the Mo d_{xy} redox orbital and the S_{ip} orbitals of the ene-1,2-dithiolate chelate portion of the pyranopterin (Figure 9). Therefore, to maintain this preferred geometry for electron transfer, final product release from the active site should only occur *after* transfer of the second electron to the 2Fe-2S cluster (**E** → **A**). This results in a fully oxidized Mo(VI) site (**A**) which is again competent to accept another substrate molecule for catalysis. Thus, electron-transfer regeneration of the active site may be said to be gated by the orientation of the Mo=O bond relative to the ene-1,2-dithiolate chelate. Finally, poor overlap between the Mo d_{xy} orbital and the S_{ip} orbitals of the ene-1,2-dithiolate in the oxidized enzyme geometry (**A**) effectively prevents premature one-electron reduction of the site by exogenous reductants, which would result in enzyme inhibition with respect to the two-electron oxidation of native substrates.

The nature of the Mo−P interaction (**C** through **E**) is currently a hotly debated issue,[6,52,53] and a detailed understanding of this interaction will provide considerable insight into the mechanism of hydroxylation in the xanthine oxidase family of enzymes. In principle, the interaction between Mo and bound product can

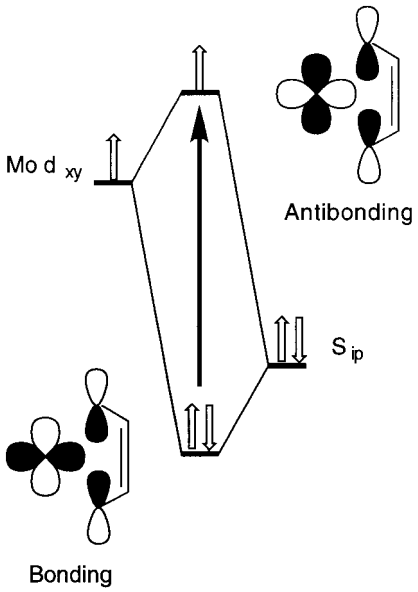

Figure 9. Partial molecular orbital diagram showing the pseudo-σ bonding and antibonding combinations of the Mo d_{xy} and dithiolate S_{ip} orbitals.

be addressed through identification of spectral features associated with CT transitions involving the Mo(V)−P complex. Previous transient absorption kinetic studies[23] of the reaction of xanthine oxidase with substoichiometric HMP under aerobic conditions have correlated the increase of the "very rapid" EPR signal with a broad absorption change (relative to oxidized enzyme) at ∼18 500 cm^{-1} (∼540 nm), and the transition was assigned as a Mo(V)−P CT transition. However, our MCD results indicate that it is the in-plane dithiolate S_{ip} → Mo d_{xy} LMCT transition which appears to be the origin of the differential absorption observed in the prior work (see Figure 9). Thus, the nature of the Mo−P interaction remains an open issue. A weak binding interaction between Mo and product leading to low-intensity CT bands and undetectable MCD cannot be ruled out, nor can we eliminate the possibility that the Mo(V)−P interaction is strong and this transition occurs in the unassigned region of the spectrum above ∼28 000 cm^{-1}.

Finally, a brief discussion of the catalytically essential sulfido ligand is warranted, since the interpretation of the MCD spectrum of the "very rapid" intermediate has been restricted to the energy region for which corresponding spectral features were exhibited by the LMoO(bdt) model compound. This spectral correspondence has resulted in new revelations concerning the geometric and electronic structure relationship between the terminal oxo ligand and the ene-1,2-dithiolate portion of the pyranopterin, as well as their synergetic roles in electron-transfer regeneration of the active site. However, the MCD spectra of the enzyme and model diverge at energies greater than 28 000 cm^{-1}. This is certainly due, at least in part, to the lack of a terminal sulfido ligand in LMoO(bdt). We therefore anticipate $S_{sulfido}$ → Mo LMCT transitions to occur at energies greater than 28 000 cm^{-1}. EPR studies of xanthine oxidase enriched with ^{33}S at the sulfido position show strong and anisotropic coupling of the ^{33}S nuclear spin to the unpaired Mo(V) electron.[19] This has been interpreted to result from a very covalent Mo d_{xy}−sulfido Sp_{π} bonding interaction, which might be expected to raise the energy of the Mo d_{xy} antibonding orbital relative to the $S_{dithiolate}$ orbitals. Surprisingly, the MCD spectrum of the intermediate shows that the sulfido ligand increases the energy of the dithiolate S_{ip} → Mo d_{xy} LMCT transition by only ∼500 cm^{-1} relative to that in LMoO(bdt).

(52) Lowe, D. J.; Richards, R. L.; Bray, R. C. *JBIC* **1998**, *3*, 557−558.
(53) Hille, R. *JBIC* **1998**, *3*, 559−560.

Currently, we are performing detailed spectroscopic studies on Mo model complexes which possess a terminal sulfido ligand in order to address this issue.

Summary

This work represents the first excited-state spectral characterization of the xanthine oxidase "very rapid" intermediate by freeze−quench difference MCD spectroscopy and has demonstrated the power of the effective spectroscopic model approach in elucidating geometric and electronic structure contributions to enzyme catalysis and electron-transfer regeneration of the active site. The virtually identical MCD spectra of the enzyme intermediate and LMoO(bdt) lead to the conclusion that the observed spectral features of the intermediate derive from a molybdenum coordination geometry where the ene-1,2-dithiolate is oriented cis to a strong-field terminal oxo ligand. Oxidized enzyme, in the absence of substrate, has been shown to possess a coordination geometry with the terminal *sulfido* ligand oriented cis to the dithiolate plane. Therefore, we have hypothesized that a conformational change occurs at the active site upon binding of the substrate. This substrate-induced conformational change allows for enhanced dithiolate $S_{ip} \rightarrow$ Mo d_{xy} covalency, providing an effective pyranopterin-mediated superexchange pathway for electron transfer between reduced Mo and an endogenous 2Fe-2S cluster hydrogen-bonded to the pyranopterin. Finally, the lack of a low-energy MCD feature clearly identifiable as a P → Mo LMCT transition in the "very rapid" intermediate is probably the result of a weakly bound Mo(V)−P intermediate leading to facile product dissociation, but the possibility also exists that the product is strongly bound and gives rise to unassigned LMCT transitions at higher energies.

Acknowledgment. We gratefully acknowledge the generous financial support of the National Science Foundation (Grant CHE-9316557), Sandia National Laboratories, and The University of New Mexico (M.L.K.), as well as the National Institutes of Health (Grant GM-057378 to M.L.K. and Grant AR-38917 to R.H.). We also thank Prof. John Enemark for helpful discussions.

IC990154J